JOURNAL OF GEOPHYSICAL RESEARCH, VOL. 115, B01101, doi:10.1029/2008JB006175, 2010

Magnetostratigraphic and rock magnetic study of the Neogene upper Yaha section, Kuche Depression (Tarim Basin): Implications to formation of the Xiyu conglomerate formation, NW China

Baochun Huang,[1] John D. A. Piper,[2] Qingqing Qiao,[1] Hailong Wang,[1] and Chunxia Zhang[1]

Received 28 October 2008; revised 3 July 2009; accepted 22 September 2009; published 13 January 2010.

[1] Magnetostratigraphic study of 251 horizons through the younger Yaha succession in the Kuche Depression of the Tarim Basin, NW China, lying beneath a massive regionally extensive (Xiyu) conglomerate formation identifies nine reversed and eight normal polarity chrons correlating with the Geomagnetic Polarity Time Scale to show that deposition spanned the interval ~5.3 to ~1.7 Ma. Sedimentation rates fell episodically from ~49 to ~24 cm/kyr as neotectonic deformation in the southern Tian Shan thrust belt became focused on two major anticlines with the northern (Qiulitage) anticline being initiated at ~5.5 Ma and developing a northern hinged limb that embraces the basal part of the studied section. Rock magnetic parameters show multiple signatures of lithologic change, deformation, burial diagenesis, and climate with the latter identifying an early Pliocene warm/humid interval followed by cooling and desertification after ~2.6 Ma. Diachronous commencement of Xiyu conglomerate deposition ranged from mid-Miocene in the north of the southern flank of the Tian Shan to Pleistocene in the south advancing as a clastic wedge derived from the uplifted range front to the north. This southward progradation was not climatically controlled although climatic effects may have modulated deposition during the Pleistocene. Uplift in the Tian Shan at ~16–15 Ma correlates with rapid increase in sedimentation rate and episodic increases occurred subsequently until the initiation of the Qiulitage anticline. Reduced rates since ~5.0 Ma contrast with increases more commonly recorded in foreland basins and have been controlled by accelerated growth of this regional structure counterbalancing uplift of the mountain front to the north.

Citation: Huang, B., J. D. A. Piper, Q. Qiao, H. Wang, and C. Zhang (2010), Magnetostratigraphic and rock magnetic study of the Neogene upper Yaha section, Kuche Depression (Tarim Basin): Implications to formation of the Xiyu conglomerate formation, NW China, *J. Geophys. Res.*, *115*, B01101, doi:10.1029/2008JB006175.

1. Introduction

[2] The Tian Shan range of central Asia (Figure 1a) is thought to incorporate two late Paleozoic sutures with ocean closure and collision leading to the amalgamation of several blocks comprising the Tarim, Yili-Central Tian Shan, and Junggar blocks [e.g., *Windley et al.*, 1990; *Gao et al.*, 1998]. Following erosion during Mesozoic and early Cenozoic times, the ancestral Tian Shan was degraded to a peneplain so that the present Tian Shan range, with peaks exceeding 7000 m and stretching ~2500 km from east to west, is predominantly a consequence of tectonic rejuvenation during the Cenozoic in response to the India-Asia collision [e.g., *Molnar and Tapponnier*, 1975; *Tapponnier and Molnar*, 1979; *Patriat and Achache*, 1984; *Avouac et al.*, 1993]. An understanding of the neotectonic (i.e., post-India-Asia collisional) deformation and uplift history of the Tian Shan range, and its surroundings is important for unravelling intracontinental deformation in central Asia induced by the India-Asia collision. It is also important for relating regional environmental changes to the global climate in response to uplift of the Himalaya, the Tibetan Plateau, and the hinterland to the north.

[3] Thick Cenozoic terrigenous sedimentary packages shed predominately from the uplifting mountain range have been deposited in foreland basins of the Tian Shan. Since accumulation rates are generally controlled by tectonics and mirror the development of the adjoining orogen, a number of magnetostratigraphic investigations have been carried out during the past decade on the Cenozoic terrigenous

[1]Paleomagnetism and Geochronology Laboratory of the State Key Laboratory of Lithospheric Evolution, Institute of Geology and Geophysics, Chinese Academy of Sciences, Beijing, China.

[2]Geomagnetism Laboratory, Department of Earth and Ocean Sciences, University of Liverpool, Liverpool, UK.

0148-0227/10/2008JB006175$09.00

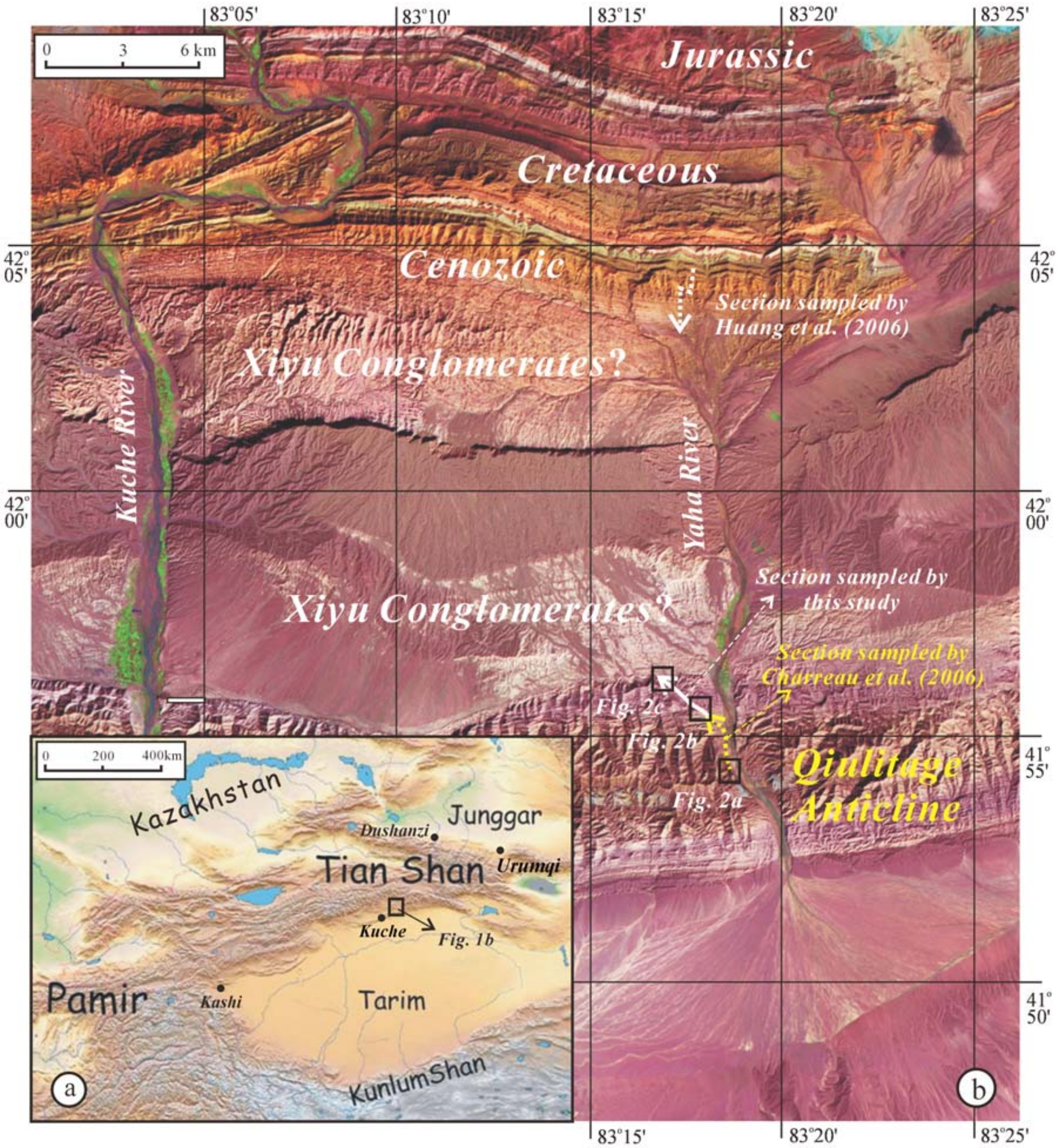

Figure 1. (a) Topographic map of the Tian Shan and its surroundings showing the tectonic framework of central Asia. (b) Landsat TM image of the Yaha section, Kuche Depression on the southern piedmont of the Tian Shan showing magnetostratigraphic sampling localities. The Jurassic, Cretaceous, and Cenozoic strata exposed in this area are distinguished approximately on the satellite image.

sequences deposited in the foreland basins of the Chinese Tian Shan [e.g., *Teng et al.*, 1996; *Yin et al.*, 1998; *Zheng et al.*, 2000; *Chen et al.*, 2002; *Sun et al.*, 2004, 2007; *Charreau et al.*, 2005, 2006, 2009; *Huang et al.*, 2006; *Heermance et al.*, 2007; *Ji et al.*, 2008; *Sun and Zhang*, 2009]. These studies have not only enabled direct age determinations to be made on these fossil-poor Cenozoic sedimentary successions, but they have also provided valuable constraints on the uplift history of the adjoining mountains, on rates of rock denudation, and on climatic change. Vigorous debates are currently ongoing and have been fuelled by limitations in the presently rather small number of study locations, but there is a general consensus that reactivation of the Tian Shan was initiated in the Oligocene and continued into early Miocene times to be succeeded by a number of rapid uplift events during Miocene and Pliocene times [*Hendrix et al.*, 1994; *Métivier and Gaudemer*, 1997; *Sobel and Dumitru*, 1997; *Yin et al.*, 1998; *Bullen et al.*, 2001, 2003; *Dumitru et al.*, 2001; *Sun et al.*, 2004; *Charreau et al.*, 2005, 2006, 2009; *Huang et al.*, 2006, 2008; *Sobel et al.*, 2006; *Ji et al.*, 2008; *Sun and Zhang*, 2009].

[4] Nevertheless many studies, primarily noting the increased component of coarse clastic deposits within the late Pliocene and Pleistocene terrigenous foreland basin successions of the Tian Shan, propose that major uplift actually occurred much later during the late Neogene era

[e.g., *Burchfiel et al.*, 1999; *Zheng et al.*, 2000; *Chen et al.*, 2002; *Fu et al.*, 2003]. The signature of this input in Xinjiang, NW China comprises a suite of dark-gray, poorly sorted, and upward-coarsening massive conglomerates and is sometimes conformable with underlying Neogene strata but elsewhere rests upon them with unconformity or paraconformity [*Bureau of Geology and Mineral Resources of Xinjiang Autonomous Region (BGMRX)*, 1993; *Jia et al.*, 2004]. This formation was originally defined as the Xiyu conglomerate formation by *Huang et al.* [1947] and ages mostly ranging from ~5 to ~1 Ma have been assigned to it from different localities around the Tian Shan based on a range of magnetostratigraphic evidence [*Teng et al.*, 1996; *Zheng et al.*, 2000; *Chen et al.*, 2002; *Sun et al.*, 2004, 2007; *Charreau et al.*, 2005; *Heermance et al.*, 2007; *Sun and Zhang*, 2009].

[5] However, the commencement of conglomerate deposition comprising the Xiyu formation remains controversial and ages as old as mid-Miocene have been estimated from the southwestern piedmont of the Tian Shan [e.g., *Sun et al.*, 2007; *Charreau et al.*, 2005, 2009; *Heermance et al.*, 2007; *Ji et al.*, 2008]. Most geological analyses interpret these massive conglomerates in terms of the latest orogenic event and regard them as an indicator of a late major uplift of the orogen in response to continuing impingement of India into Asia [e.g., *Huang et al.*, 1947; *Li et al.*, 1979; *Zheng et al.*, 2000]. In contrast, some other studies propose that conglomerate deposition was controlled by increasing rates of erosion resulting from the influence of climate change [e.g., *Avouac et al.*, 1993; *Burchfiel et al.*, 1999; *Zhang et al.*, 2001]. In particular, when *Sun et al.* [2004, 2007] determined a basal age of ~2.58 Ma from a late Neogene succession in the northern Tian Shan according with the onset of large ice sheet formation in high northern latitudes they proposed that: "climatic cooling rather than tectonics has played a dominant role in producing the thick Xiyu conglomerates."

[6] Hitherto the basal age of the Xiyu conglomerate formation has generally been estimated from the magnetostratigraphic age of the top of the underlying terrigenous sediments since there are only a few interbedded mudstone and siltstone layers near the base of the Xiyu conglomerates suitable for paleomagnetic study. Thus, whether or not there is a large sedimentary break between the Xiyu conglomerates and the underlying sequence controls the reliability of the basal ages determined for conglomeratic input. The underlying late-Miocene to Pliocene terrigenous sediments in the foreland basins of the Chinese Tian Shan, namely the Kuche (Kuche Depression), Atushi (Kashi Depression), and Dushanzi formation (southern margin of the Junggar Basin), are generally characterized by yellow-brown sandstone, siltstone, and mudstone in the lower part and upwardly more frequent thin conglomerate interbeds in the higher parts of the succession [*BGMRX*, 1993; *Jia et al.*, 2004].

[7] Although this succession is readily distinguished from the overlying dark-gray massive Xiyu conglomerates, the presence of thin conglomerate interbeds has formerly led to a lack of clarity in definition of the base of the Xiyu formation. In the magnetostratigraphic study on the Yaha section, *Charreau et al.* [2006] state that "the series becomes progressively coarser grained toward the top, until reaching a thick gray conglomerate unit, which likely belongs to the Xiyu formation." Recent re-evaluation of the Yaha section [*Huang et al.*, 2008] has found that the top of their section actually correlates approximately with the boundary of the Kangcun and Kuche formations, and a large thickness of ~1200 m of the Kuche formation intervenes between the top of the succession studied by *Charreau et al.* [2006] and the base of the Xiyu formation. Thus detailed magnetostratigraphic study of the succeeding late Neogene sequence in the foreland basins of the Tian Shan has proved essential for constraining the basal age of the Xiyu conglomerates in this region and for resolving whether this formation is a signature of neotectonics or of climate change.

[8] In this study, we report a magnetostratigraphic study of the youngest part of the succession lying beneath the Xiyu conglomerates and above the level investigated by *Charreau et al.* [2006]. We have aimed thereby to clarify the basal age of the Xiyu conglomerate deposition in this region and also to evaluate long-term climate changes from rock magnetic investigation to resolve whether climatic control was an important factor in its formation. From comparison of the long-term climate changes resolved in this succession and from the late Neogene Kuitun He section in the northern piedmont of the Tian Shan [*Sun et al.*, 2007], it becomes possible to derive a conceptual model for the emplacement of the Xiyu conglomerates in the Chinese Tian Shan.

2. Geological Background and Sampling

[9] As one of two major Cenozoic depocenters along the northern margin of the Tarim Basin [*BGMRX*, 1993; *Métivier and Gaudemer*, 1997; *Yin et al.*, 1998], the thick Cenozoic terrigenous sediments in the Kuche Depression have been repeatedly studied during the past decade [*Teng et al.*, 1996; *Yin et al.*, 1998; *Charreau et al.*, 2006; *Huang et al.*, 2006, 2008] and the Yaha section partly investigated by *Charreau et al.* [2006] is located in the north of the town of Yaha, Kuche County where the south-flowing Yaha River cuts the box-like Qiulitage (or Qiulitak) anticline; the study section of these authors is located in the northern limb of this anticline and is separated from our 2006 sampling section by a N–S distance of some 10 km (Figure 1b). The base of the Yaha section comprises interbedded gray-green to green sandstones (Figure 2a) with an age commencing at ~12.6 Ma [*Charreau et al.*, 2006] and probably belongs to the upper part of the Neogene Jidike formation in the Kuche Depression [*BGMRX*, 1993]. These sandstones are overlain successively by the Kangcun and Kuche formations. In the upper part of the section, the Kuche formation is characterized by gray-yellow mudstones, siltstones, and sandstones with interbedded thin conglomerates and is compatible with the type Kuche formation [*BGMRX*, 1993; *Jia et al.*, 2004]. The Kuche formation in the Yaha section has a thickness of over 1000 m and is covered by a suite of dark gray conglomerates without significant change in bedding attitudes (Figures 2c and 2d), indicating a conformable contact and suggesting no protracted pause in deposition between the Neogene Kuche formation and the overlying Xiyu conglomerates.

[10] Sedimentation in this sector of the southern Tian Shan thrust belt has been concurrent with ongoing neo-

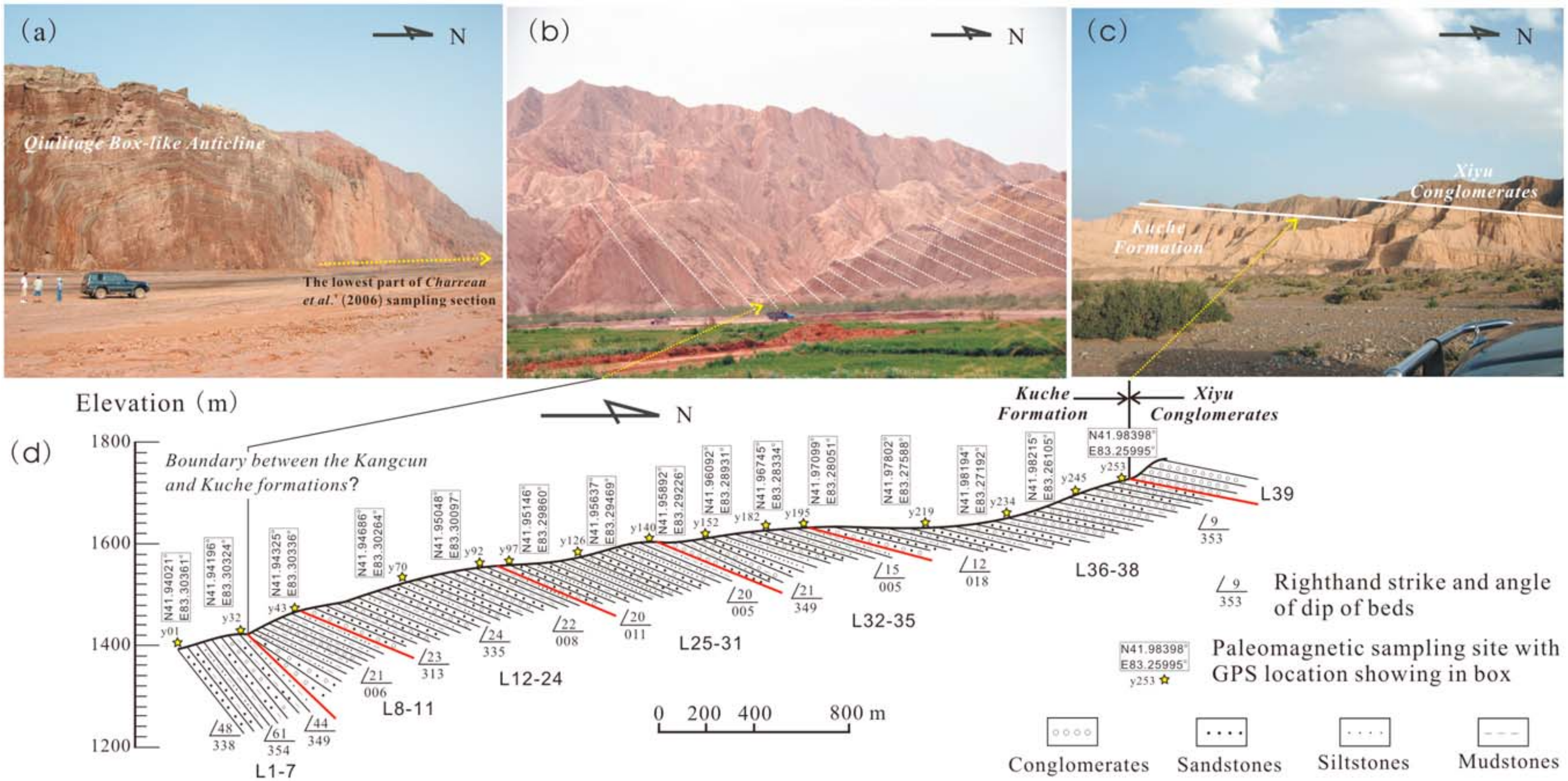

Figure 2. (a) Photograph showing northern limb of the Qiulitage box-like anticline in the vicinity of the fold axis. (b and c) Photographs showing successive contact within the Kangcun/Kuche formations (layers 7 and 8) and the Kuche/Xiyu conglomerate formations (layers 38 and 39) at the upper Yaha section. (d) Cross section of the late Neogene succession lying above the level investigated by *Charreau et al.* [2006] and exposed in the northern limb of the Qiulitage anticline; layered stratified units L1–39 distinguished in the field are shown and the sampled horizons comprise layers 1–38.

tectonism, and high-level deformation has been focused on two major folds: the Yakeng anticline is a detachment fold displaying incremental uplift and rotation of the fold limbs while the Qiulitage anticline ~10 km to the north is a complex fault bend fold incorporating a back thrust abutting an angular limb to the north and a kink band to the south which has migrated progressively upward since ~5.5 Ma [*Hubert-Ferrari et al.*, 2007]. The sampled section spans a thickness of 1177 m (Figures 1b and 2d) and crosses the outcrop of the northern angular limb of this fold (Figure 2a); it succeeds the section investigated by *Charreau et al.* [2006] with ~77 m of overlap. Lithostratigraphic evaluation of the upper part of the Yaha section identifies 39 layers divided by prominent bedding planes with thicknesses ranging from several meters up to ~160 m (Figures 2d and 3). Bedding attitudes range from 40° to 60° to the north in the first seven divisions; tilt in the higher levels is smaller and decreases to ~10° toward the north in divisions L36–39 (Figures 2b, 2c and 2d). The major change in bedded attitude occurs between layers 7 and 8 (Figure 2b) and records the passage across the axial plane of the northern box-like limb; it also correlates approximately with the boundary between the Kangcun and Kuche formations. In total, 253 horizons were selected for paleomagnetic sampling and two oriented drill-cores were collected from each horizon using a portable petrol-powered drill. Sampling intervals are typically separated by 2–5 m between successive horizons but are sometimes as large as ~10 m where the sequence is composed mostly of conglomerate or coarse sandstone. All the drill-cores were oriented by magnetic compass. A local declination of 3° determined from the present International Geomagnetic Reference Field in the sampling area was used for correcting drill-core azimuths and bedding attitudes.

3. Paleomagnetism and Magnetostratigraphic Results

[11] Cylindrical specimens ~2 cm in length were cut from field samples and nine pilot specimens from different levels were selected for measurement of successive acquisition and backfield demagnetization of isothermal remanent magnetization (IRM). The results (Figure 4) show quasi-saturation behavior by 0.2–0.5 T followed by further gradual increase in IRM intensity up to 2.7 T and remanent coercivities ranging from ~50 to 90 mT. Combined with thermal demagnetization behaviors (Figure 5), IRM acquisition and backfield demagnetization results identify both magnetite and hematite as remanence carriers. Thus, magnetominerology is comparable to the Neogene terrigenous sediments previously sampled in the Kuche Depression and elsewhere in the foreland basins of the Tian Shan [e.g., *Charreau et al.*, 2005, 2006; *Huang et al.*, 2004, 2006].

[12] At least one specimen per horizon was subject to progressive thermal demagnetization in a TD-48 thermal demagnetizer with temperature intervals of 50 or 100°C to 500°C and of 30 or 20°C as the maximum unblocking temperatures of the remanence carriers were approached. Magnetizations were measured by a 2G-760R U-channel system and performed in a magnetically shielded room with field minimized to <300 nT. Demagnetization results were evaluated on stereographic projections and orthogonal diagrams [*Zijderveld*, 1967] with the latter used to resolve component structures using principal component analysis [*Kirschvink*, 1980].

[13] Similar to the approach, we have used to resolve the Oligocene and Neogene magnetostratigraphy in the Kuche Depression [*Huang et al.*, 2006], two rounds of progressive thermal demagnetization were performed with the second round of demagnetization performed on horizons that initially showed erratic or anomalous high-temperature trajectories. In general, most progressively demagnetized specimens show relatively straightforward trajectories toward the origin of orthogonal plots following removal of a viscous or low-temperature component (LTC) by temperature steps of 200–300°C (Figure 5). The LTC is predominantly of normal polarity and only one out of 118 specimens in which it could be resolved by three or more temperature steps showed reversed polarity. The LTC components cluster around the present geomagnetic field (PGF) in geographic coordinates and significant deterioration in directional grouping follows complete unfolding (Figure 6a).

[14] In contrast, the characteristic remanent magnetization (ChRM) is of dual polarity and mostly subtracted at temperature steps between 200 and 300°C and 670–690°C (Figures 5a, 5b, 5e, and 5i), and less commonly between 200 and 400°C and 590–620°C (Figure 5c and 5d). This demagnetization behavior conforms to the IRM acquisition and backfield demagnetization results and identifies both magnetite and hematite as remanence carriers. In total, 256 out of 264 demagnetized specimens, selected from 251 sampled horizons (samples from 2 of 253 sampled horizons were spoiled in transportation), could isolate stable ChRM from four or more temperature steps. Maximum angular deviations (MAD) [*Kirschvink*, 1980] are mostly less than 10° with just five ChRMs having values from 10 to 14°. The 256 ChRM directions yield an overall mean of D = 359.5°, I = 75.1° (k = 11.8, α_{95} = 2.7°) before and D = 357.6°, I = 54.1° (k = 14.0, α_{95} = 2.4°) after tilt adjustment and identify marginal improvement in directional grouping following complete unfolding (Figure 6b). The reversal test [*McFadden and McElhinny*, 1990] is positive with an angular difference of 2.7° between tilt-corrected overall mean directions of each polarity; this is less than the critical angle of 4.9° at the 95% confidence level and yields a class A reversal test. Collectively, relatively straightforward demagnetization trajectories, significant difference between the overall mean direction and the PGF (Figure 6b), and the positive reversal test indicate that the ChRMs were acquired at, or close to, the time of rock formation and can be interpreted as essentially primary in origin.

[15] The ChRM directions were used to calculate virtual geomagnetic pole (VGP) latitudes, and the section organized into stratigraphic levels referred to these latitudes (Figure 3) in order to define magnetic polarity zones. Excluding two zones suggested from one horizon only, a total of eight normal (N1–N8) and nine reversed (R1–R9) polarity zones are clearly identified (Figure 3). This magnetic polarity sequence can be readily correlated with chrons C1r.2r to C3r of the ATNTS2004 Geomagnetic Polarity Time Scale (GPTS) [*Lourens et al.*, 2004] based upon the following observations:

[16] 1. Field lithologic inspection indicates that the base of the section correlates with the boundary between the

Kangcun and Kuche formations in the Kuche Depression with previous work suggesting a magnetostratigraphic age of ~6 Ma for this boundary [*Huang et al.*, 2006].

[17] 2. The sampled section is characterized by siltstones, mudstones, coarse-grained sandstones, and upwardly more frequent thinly interbedded conglomerates (Figures 2d and 3) compatible with the type Kuche formation in the depression [*BGMRX*, 1993; *Jia et al.*, 2004]. Although biostratigraphic constraints are poor, previous magnetostratigraphic studies indicate that this formation, as well as its counterparts in the Kashi Depression (Atushi formation) and the northern piedmont of the Tian Shan (Dushanzi formation), is dominated by a long reversed polarity zone believed to correlate with the Gilbert reversed chron [*Teng et al.*, 1996; *Zheng et al.*, 2000; *Sun et al.*, 2004; *Charreau et al.*, 2005; *Sun and Zhang*, 2009].

[18] 3. The middle and lower parts of the polarity sequence are dominated by a relatively thick reversed zone (R5) at ~500–730 m preceded by four pairs of normal and reversed polarity zones (N5–R9); this pattern of magnetozones is readily correlated with chrons C2Ar to C3r of the ATNTS2004. In the upper part of the section, the well-established magnetozones at ~730–1150 m are characterized by a pair of relatively thick reversed and normal polarity zones (R2 and N2) and two pairs of relatively short normal and reversed zones (R3 and N4) which correlate well with chrons C2r to C2An.3n of the ATNTS2004; the top of the section (R1 and N1) correlates with the base of chrons C1r.2r and C2n of the ATNTS2004. The number of reversals and their relative thicknesses accordingly indicate that the upper Yaha section was deposited between ~5.3 and ~1.7 Ma and that the conformably overlying Xiyu conglomerates have an early Pleistocene age of ~1.7 Ma at their base (Figure 3).

[19] The base of the section overlaps with the top of the section studied by *Charreau et al.* [2006] by ~77 m, and our magnetostratigraphy indicates that this part comprises a pair of normal and reversed magnetozones (lower N8 and R9) with a polarity transition occurring at the ~45 m level (Figure 3). We correlate this with the boundary between chrons C3n.4n and C3r of the ATNTS2004; the results of the two studies are thus in conformity because the top ~23 m of the section studied by *Charreau et al.* [2006] has also been estimated to belong to the polarity transition between chrons C3n.4n and C3r. The sediment accumulation rate below the ~730 m level resolved from a plot of magnetostratigraphic age versus height within our section yields an average sedimentation rate of ~42 cm/kyr (Figure 7) which is not significantly different from the estimate for the middle and upper parts of the section studied by *Charreau et al.* [2006] (~43 cm/kyr); these values are at the higher end of typical sedimentation rates estimated from foreland-basin environments (10–40 cm/kyr) [*Burbank et al.*, 1992; *Harrison et al.*, 1993]. Hence magnetostratigraphic ages resolved in this study and the one by *Charreau et al.* [2006] imply that the whole Yaha section in the Kuche Depression was deposited between ~12.6 and ~1.7 Ma with massive Xiyu conglomerate deposition not commencing here until the early Pleistocene (GTS2004 geological time scale, *Gradstein et al.* [2004]). The upper part of our section above the ~730 m level has a relatively lower sedimentation rate averaging ~24 cm/kyr (Figure 7). We evaluate the significance of these sedimentation rates in section 5.1.

4. Rock Magnetism, Long-Term Climate Change and Diagenesis

[20] To further explore depositional environments and long-term climate changes in the study region, 249 specimens from the sampled 253 horizons were subject to measurement of anisotropy of magnetic susceptibility (AMS) employing a KLY-3 kappabridge before thermal demagnetization. A parallel suite comprising 236 specimens from the 253 horizons was subject to rock magnetic investigation of (1) both low- and high-frequency magnetic susceptibilities using a Bartington MS2 magnetic susceptibility system, (2) saturation isothermal remanent magnetization (SIRM) produced in a steady constant field of 2.7 T and the residual SIRM remaining after application of a 300 mT backfield demagnetization (designated $SIRM_{-300mT}$ hereafter), and (3) anhysteresis remanent magnetization (ARM) produced in a steady direct current field of 0.05 mT applied to an alternating field demagnetization with peak field of 100 mT. The SIRM and $SIRM_{-300mT}$ were imparted by 2G-660 pulse magnetizer and measured by JR-5 spinner magnetometer; ARM acquisition and magnetic measurements were performed using a 2G-760R U-channel system coupled with a Model 2G600 automatic sample degaussing system situated in a magnetically shielded room.

[21] The AMS results show that the fabric shapes are predominantly oblate with low corrected degrees of anisotropy (P_j) in the range of 1.02–1.05; in the upper part of the section above ~730 m in height, magnetic fabrics become more neutral to prolate in shape with relatively low P_j values (Figure 8a). Minimum principle anisotropy directions (k_3) are generally oriented perpendicular to bedding in stratigraphic coordinates with specimens from the upper part of the section above ~730 m in height showing slight southward inclination; in contrast maximum principle anisotropy directions (k_1) are all nearly horizontal and trend marginally SW and NE of an E–W axis (Figure 8b). The southward imbrication of magnetic fabrics in more neutral to prolate particles in the upper part of the section is probably the response to southward current flow [e.g., *Tarling and Hrouda*, 1993], suggesting that the magnetic fabric is primary and controlled by sedimentation. A similar distribution of k_3 axes is also observed in the Pliocene Dushanzi formation in the Kuitun He section in the northern piedmont of the Tian Shan; in this latter case a slight northward inclination of the k_3 axes suggests northward imbrication of magnetic particles induced by northward flow debouching from the Tian Shan (see Figure 7b of *Sun et al.* [2007]). However, the tight grouping of k_1 axes, the greater importance of oblate fabrics, and the absence of imbrication in the lower part of the succession are comparable with our previous studies in older members of this sedimentary basin [*Huang et al.*, 2006, 2008]. While the transition from prolate/neutral to oblate fabrics and some reduction in imbrication with depth could be explained by the effects of compaction, the grouping of k_1 axes is less readily explained in this way and suggests a response to incipient deformation in the foreland basins of the Tian Shan induced

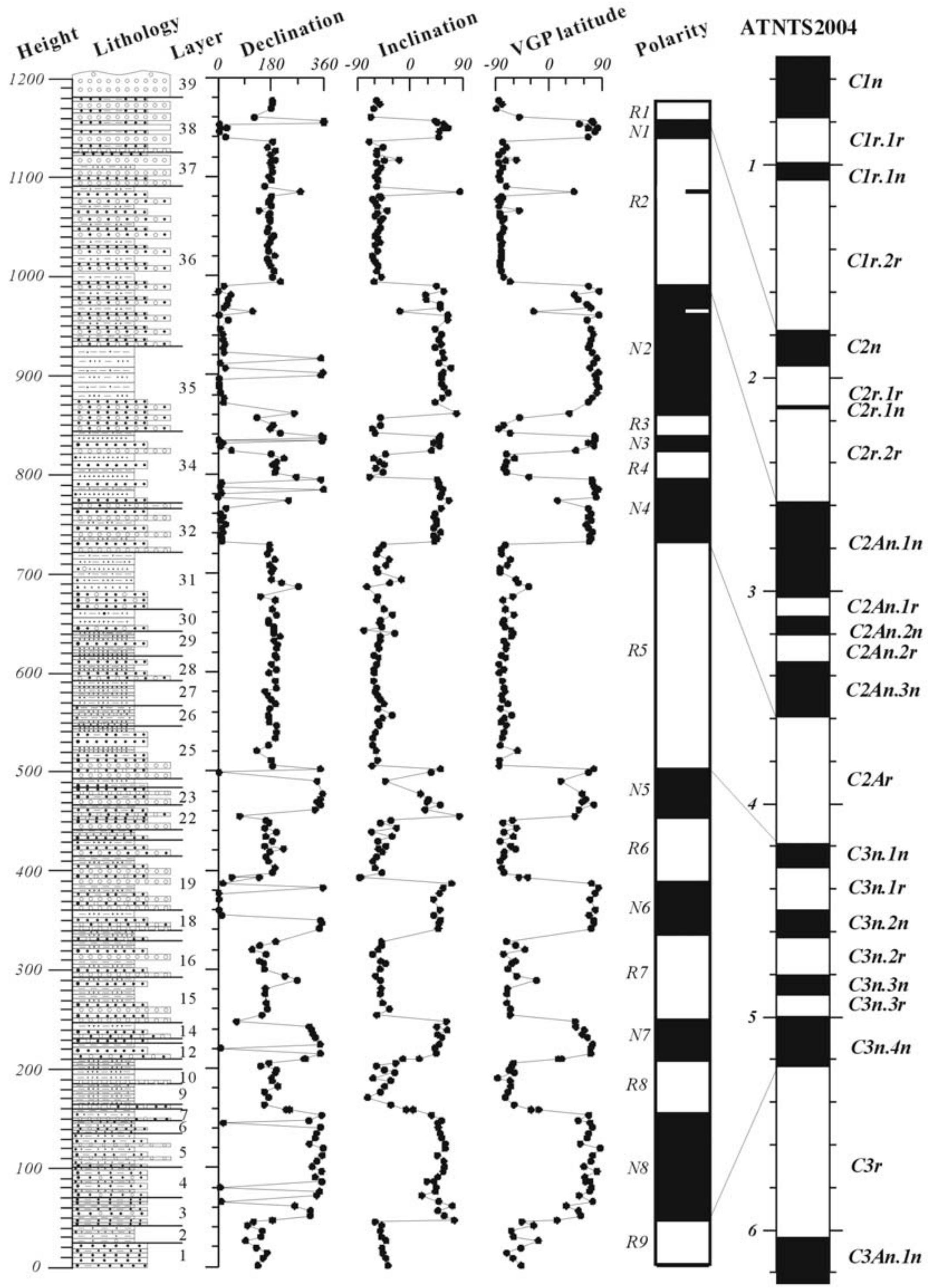

Figure 3. Lithology log and magnetostratigraphic results from the upper Yaha section in the Kuche Depression, NW China. The characteristic remanence declination and inclination and VGP latitude are plotted as a function of stratigraphic level and the correlation with the ATNTS2004 geomagnetic polarity time scale [*Lourens et al.*, 2004] is shown. Two magnetochrons defined by only one horizon are shown by short-half bars. Lithologic legends are the same as for Figure 2d.

by the ongoing N–S compression and crustal shortening estimated to be occurring at rates of 0.5–1.0 mm/yr [e.g., *Hubert-Ferrari et al.*, 2007]. This secondary influence of progressive strain mirrors the effects of AMS ellipsoid evolution in sediments subject to progressive deformation [*Parés*, 2004].

[22] Figure 9 shows the rock magnetic results plotted as a function of stratigraphic level. Within the natural dispersion

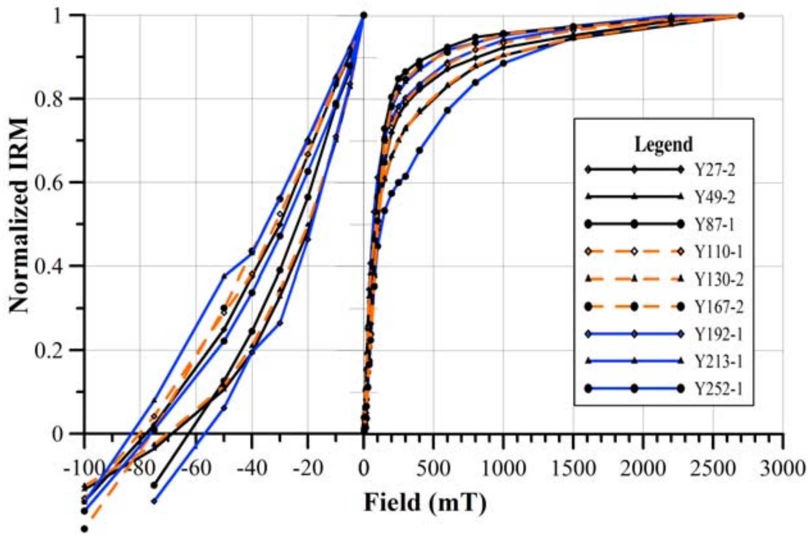

Figure 4. Behavior of acquisition and backfield demagnetization of isothermal remanent magnetization (IRM) for pilot samples from representative horizons in the upper Yaha section, Kuche Depression.

of these parameters between levels, we recognize several systematic trends here. First, there is a progressive increase in k_{lf}, k_{fd}% and ARM in the sediments beneath the axial plane of the box fold comprising the northern limb of the Qiulitage fold (Figures 9a, 9c, and 9e). This fold reaches the surface between levels 7 and 8 corresponding to the lithologic change between the gray-green sandstones of the Kangcun formation and the gray-yellow mudrocks and sandstones of the Kuche formation. Collectively these signatures are attributable to lithologic changes reflecting an increasing input of SP, SD, and PSD ferrimagnetic particles into the succession anticipating the deposition of the Kuche deposition at ~5 Ma. The absence of abrupt changes in rock magnetic properties at this point also indicates that no significant hiatus occurred at this time (Figure 9 and see also section 5.1).

[23] The increase in k_{fd}% in the lower part of the succession and decrease in the upper part (Figure 9c) are potential paleoclimatic signatures. The parameter k_{fd}% is a measure of the percentage difference between the readings at high and low frequencies where $k_{\mathrm{fd}}\% = [(k_{\mathrm{lf}} - k_{\mathrm{hf}})/k_{\mathrm{lf}}] \times 100$ and k_{lf} and k_{hf} are the corrected readings of susceptibility at low (0.47 kHz) and high (4.7 kHz) frequencies, respectively. SP grain sizes in ferrimagnetic minerals <30 nm in size have contrasting susceptibilities at these frequencies whereas grains >30 nm in size show no differences [*Dearing et al.*, 1966]. This response occurs because SP grains oscillate at low frequencies but are unable to follow high-frequency changes and keep in phase with the applied field; for k_{fd}% values <5% SD, PSD, and MD grain sizes dominate whereas for k_{fd}% >5% SP grains dominate. In this collection, k_{fd}% values are low (<3%) confirming the importance of the SD and PSD component, but there is a distinct increase of k_{fd}% to ~5% within the middle part of the section between ~480 and ~730 m (Figure 9c) with an assigned magnetostratigraphic age of ~4.2–3.6 Ma. This portion of the succession is evidently characterized by enhanced contents of SP particles, and this seems to reflect an increase in the intensity of chemical weathering during early Pliocene times contemporaneous with a remarkable warm/humid climate event that occurred during early Pliocene times in East Asia [*Hoorn et al.*, 2000; *Wang et al.*, 2001; *Wu*, 2001; *Li et al.*, 2005; *Sun et al.*, 2007].

[24] Further grain size variations in the magnetite content may be recognized by a plot of anhysteretic susceptibility (k_{ARM}) versus low-field susceptibility (k_{lf}) (Figure 10). In general, k_{ARM} is sensitive to the SD and smaller PSD magnetite grains whereas k_{lf} responds more to the larger PSD and MD grains [*King et al.*, 1982]. The lowest and highest levels in the succession (circles and squares in Figure 10) show a bias toward coarser grain sizes while the ~480–730 m level (triangles) shows a bias toward finer grain sizes. Hence similar height-depended variations of k_{fd}%, ARM, ARM/SIRM, and ARM/k_{lf} between ~156 and 990 m in Figures 9 and 10 (i.e., within the interval ~5.0–2.6 Ma) are presumably modulated by grain sizes variations in the magnetite (Figures 9c, 9e, 9g, 9h, and 10). The first shows an abrupt fall corresponding to the reduction in sedimentation rate at ~730 m dated ~3.6 Ma whereas the latter three are somewhat longer term trends and possible proxies for the climatic deterioration during late Pliocene and early Pleistocene.

[25] The SIRM ratio (S) in the form of SIRM$_{-300\ \mathrm{mT}}$/SIRM, which is likely to be in part a significant indicator of magnetite-to-hematite ratio, shows a long-term trend of up-section increase from ~0.5 at the base to ~0.7 at the top (Figure 9b) on which are superimposed shorter term variations. Specifically, the lowest values are recorded in the central part of the succession highlighted above as the interval recording chemical weathering, and these are likely to be the signature of a pedogenic hematite component. The longer term increase in this parameter probably reflects a progressive response to lithification and diagenesis associated with fluid migration and expulsion. Hematite formation by diagenesis might occur by incipient alteration of the detrital magnetite or conversion from paramagnetic silicates (or both) and could decrease the S parameter but have no perceptible effect on the paleomagnetic record if grain size fractions smaller than SD are produced. A signature of burial diagenesis should be resolvable from climatic and

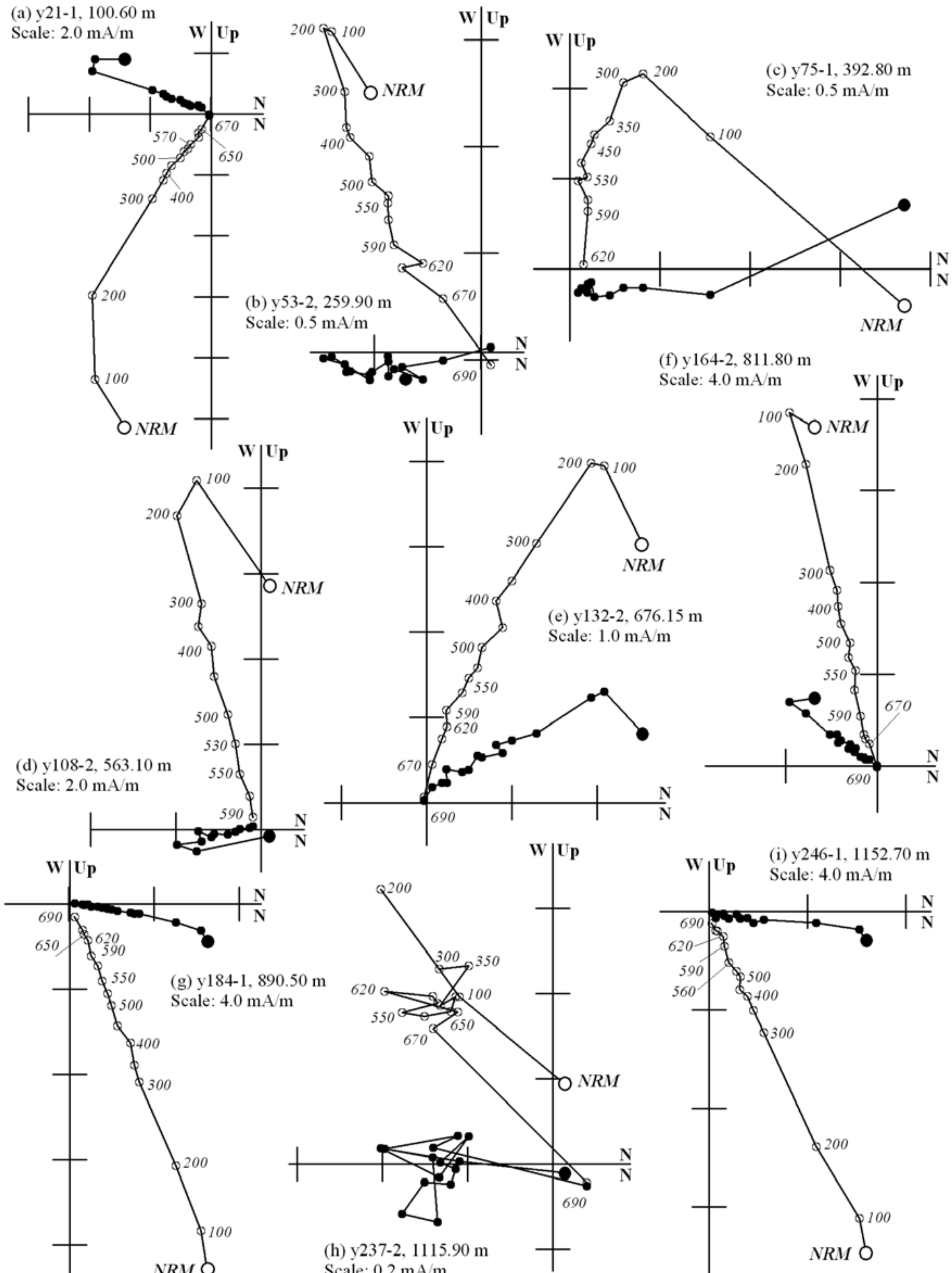

Figure 5. Orthogonal [*Zijderveld*, 1967] vector plots of representative specimens from different levels in the upper Yaha section. Directions are plotted in situ; solid and open circles represent vector endpoints projected onto horizontal and vertical planes, respectively.

lithologic changes by being progressive through the succession and (with the exception of the fabric parameters noted above) only the S-ratio seems to suggest this; all the other rock magnetic parameters show different trends in the lower part of the succession from the upper part and hence no profound signature of diagenesis.

[26] The complex interrelationship of climatic, sedimentologic, and diagenetic factors controlling magnetic proper-

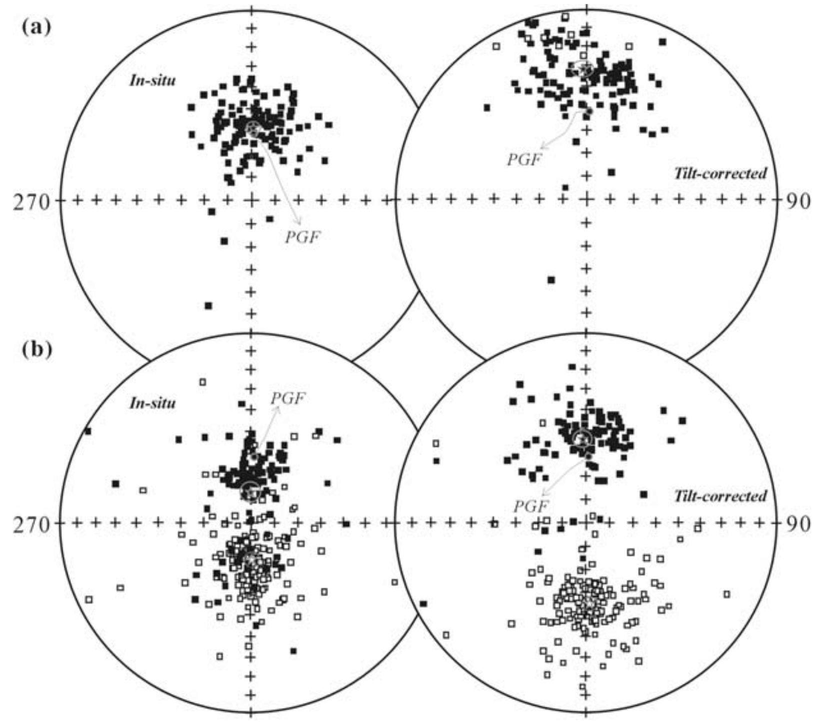

Figure 6. Equal-area projections of remanence directions from sampled horizons and overall mean directions (stars) with 95% confidence ellipses before and after tilt correction: (a) The 118 directions of low unblocking temperature remanent magnetizations; (b) the 256 directions of high-temperature characteristic remanent magnetizations. Solid/open symbols represent downward/upward inclinations; PGF indicates the direction of present geomagnetic field.

ties renders the isolation of any single cause is a difficult task. However, the protracted interval characterized by consistently high and fairly uniform values of k_{fd}%, ARM, ARM/SIRM, and ARM/k_{lf} falls within the interval ~5.0 and 3.6 Ma (Figure 9) and probably reflects climatic influence most closely because it corresponds to the warm/humid epoch that occurred during early Pliocene times in East Asia [*Hoorn et al.*, 2000; *Wang et al.*, 2001; *Wu*, 2001; *Li et al.*, 2005; *Sun et al.*, 2007]. In the longer term, NW China has been dominated by an arid continental climate with moderately high temperatures accompanied by short periods of limited summer rainfall at least since formation of the Taklimakan Desert in the Tarim Basin at ~5.3 Ma [*Sun and Liu*, 2006]. Given that late Neogene sediments of the foreland basins were mainly shed from the Tian Shan during mountain uplift, the source of the late Neogene sediments might be expected to have a similar provenance and yield comparable ferromagnet compositions. In this case, changes in k_{fd}%, ARM, ARM/SIRM, and ARM/k_{lf} parameters would reflect the changing balance of physical to chemical weathering responding to degrees of aridification and cooling in the source region [*Balsam et al.*, 2004]. The fall in k_{fd}% and ARM in this highest part of the succession records reductions in SP and SD grain populations, respectively; parallel reductions in ARM/SIRM and ARM/k_{lf} after ~2.6 Ma further suggest that larger grain size fractions make up the overall magnetic grain population (Figure 10). These signatures are presumably a collective response to the enhanced physical weathering during the Pleistocene Epoch with the strengthening aridification and cooling in NW China [e.g., *An et al.*, 2001; *Guo et al.*, 2002; *Sun and Liu*, 2006; *Dupont-Nivet et al.*, 2007]. The specific causes are likely to be complex and involve both changes in detrital magnetite grain sizes and reduction in hematite derived from pedogenic processes. We also stress that these observations relate to the clastic layers of finer grain size appropriate to paleomagnetic investigation and are not necessarily applicable to the intercalated rudaceous layers.

5. Discussion

5.1. Sedimentation Rates and Late Neogene Deformation by Folding in the Study Region

[27] As noted above and shown in the cross section of Figure 2d, there is significant reduction in tilt between layers 7 and 8 crossing the angular box-like feature defining the northern limb of the Qiulitage anticline. This is a growth fold expanding to approximately four times its surface width at 5 km depth [*Hubert-Ferrari et al.*, 2007], and syntectonic deformation was evidently already controlling sediment input near the base of the sampled succession by ~5 Ma. Three observations are relevant to interpretation of this part of the succession: (1) the first seven layers have 45–60° angles of dip according approximately with bedding attitudes of older strata exposed on the northern limb of the Qiulitage anticline (i.e., above ~2660 m in the section studied by *Charreau et al.* [2006] where dips range between ~40 and ~70° but are predominantly 50–60°); in contrast layers L8–39 have successively decreasing dips from ~20°

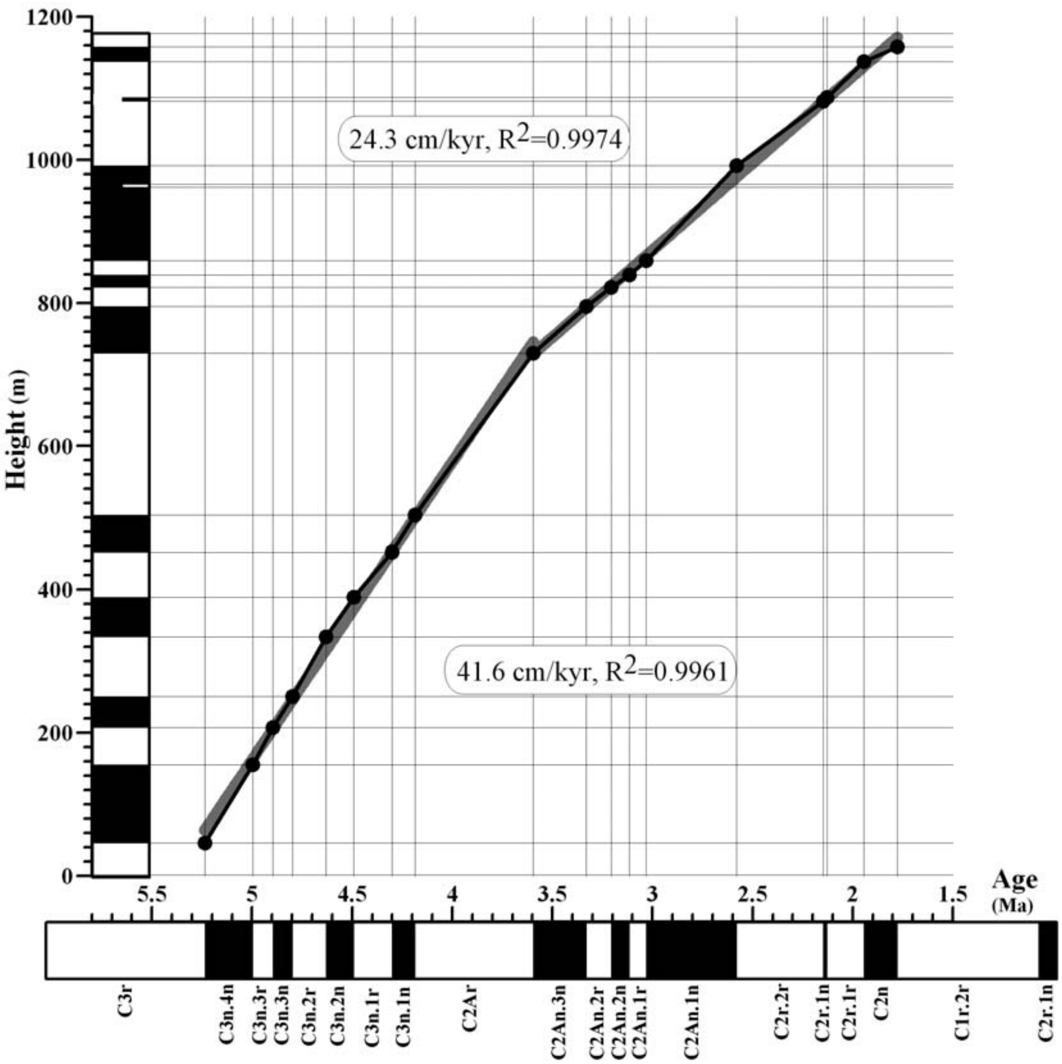

Figure 7. Stratigraphic height as a function of magnetostratigraphic age in the upper Yaha succession of the Kuche Depression showing accumulation rates in the studied section. Age constraints are determined by correlating the polarity chrons (*y* axis) with the ATNTS2004 geomagnetic polarity time scale [*Lourens et al.*, 2004] as shown in Figure 3.

in layers L8–11 to ~10° at the top of the studied section (Figures 2b and 2d); (2) layers L6–7 and L8–9 in the top Kangcun formation and basal Kuche formation comprise similar upward-coarsening cyclothems (Figures 2b, 2d, and 3); (3) sedimentation rates resolved from the plot of stratigraphic height versus magnetostratigraphic age are approximately consistent from the base to the ~730 m level (Figure 7) and compatible with results from the underlying succession in the middle and upper parts of the section studied by *Charreau et al.* [2006]. Observations 2 and 3 indicate that no significant breaks in sedimentation occurred at this level and no significant hiatus is evident in the higher succession; however, growth of the Qiulitage anticline at this point is evidently younger than layer 8 (~5.5 Ma and see also *Hubert-Ferrari et al.* [2007]) and may be expected to have influenced subsequent sedimentation rates.

[28] The sediment accumulation rate below the ~730 m level resolved from a plot of magnetostratigraphic age versus height within our section is ~42 cm/kyr (Figure 7) comparable with the middle and upper parts of the section studied by *Charreau et al.* [2006] (~43 cm/kyr). We adopt a conservative assessment in Figure 7 although a small reduction in sedimentation rates at the 340 m level (~4.6 Ma) is apparent and equivalent to a sediment input averaging ~49 cm/kyr falling later to ~38 cm/kyr and suggesting that sedimentation may have increased during initiation of the Qiulitage anticline. In contrast, the upper part of the section above the ~730 m level exhibits a relatively lower sedimentation rate averaging ~24 cm/kyr between ~3.6 and 1.8 Ma (Figure 7). The episodic reduction in sedimentation rate through this succession prior to Xiyu conglomerate deposition (Figure 7) may seem inconsistent with generally increasing sedimentation rates during the late Neogene times in some other parts of central Asia and resulting from increased input of coarse clastics during the Pleistocene [e.g., *Burchfiel et al.*, 1999; *Chen et al.*, 2002; *Fu et al.*, 2003; *Sun et al.*, 2004; *Charreau et al.*, 2005, 2006; *Huang et al.*, 2006]. Nevertheless, this kind of punctuation in sedimentation rate is repeatedly observed in the Neogene sequence in the Jingou He section on the northern piedmont

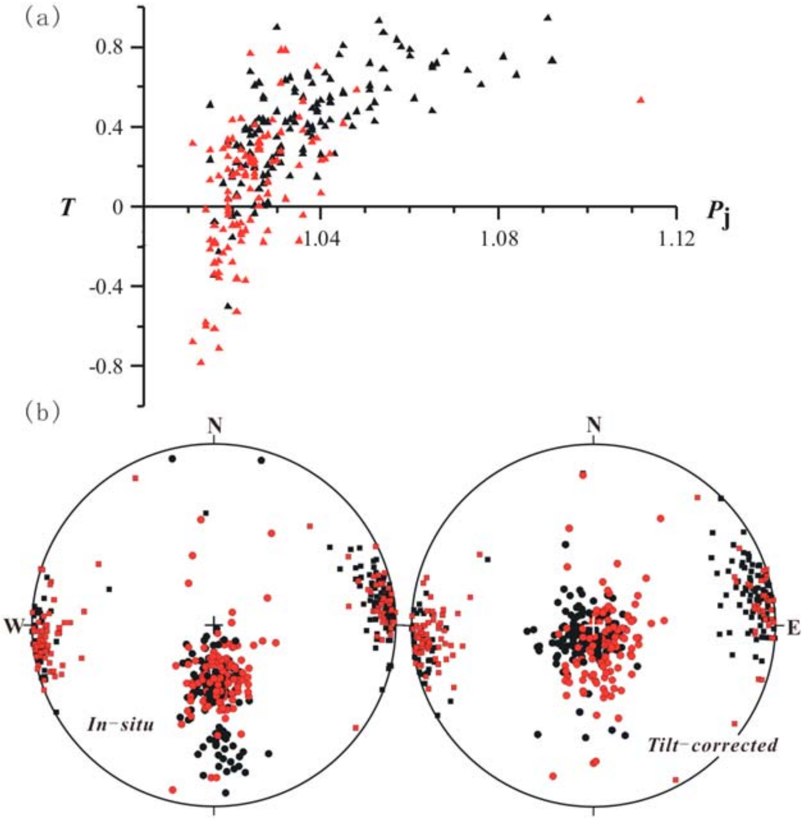

Figure 8. Summary of AMS results from the upper Yaha section of the Kuche Depression, NW China. (a) P_j–T (corrected AMS degree versus AMS shape parameter) plot. (b) Stereographic projections (lower hemispheres) of AMS orientations before and after tilt correction; squares and circles show orientations of maximum and minimum principle axes of magnetic susceptibility, respectively. Black and red symbols indicate AMS data from below and above the ~730 m level, respectively.

of the Tian Shan where alternations in sedimentation rate have been linked to punctuated uplift of the adjoining source region [*Ji et al.*, 2008]. Although lithostratigraphy can often be correlated well from place to place, it has been observed that the complexity of sedimentation in foreland basins and the multiple progradation of high-energy flood systems encroaching upon ephemeral lakes can result in markedly contrasting sedimentation rates within the same depositional system [e.g., *Heermance et al.*, 2007; *Sun et al.*, 2007].

[29] Prior to sedimentation of the succession studied here, thrusting and folding in the Kuche Depression have involved successive reactivation of folding and crustal shortening. In these circumstances, sedimentation then provides a proxy for fold and thrust development [e.g., *Burbank et al.*, 1996] and indicates that the Tian Shan has been subjected to a multiple episodic uplift history at ~16, ~11, ~7–5 Ma following initiation at ~20 Ma [e.g., *Sun et al.*, 2004; *Charreau et al.*, 2005, 2006, 2009; *Huang et al.*, 2006, 2008; *Ji et al.*, 2008, and this study]. The assumption of a constant sedimentation rate between 10 Ma and the present [*Hubert-Ferrari et al.*, 2007], however, is clearly in need of revision and implies, on the contrary, that sedimentation rate in this region is controlled by local tectonic effects linked to basement flexure and sediment supply. These latter authors describe an emergence and accelerated uplift of the Qiulitage anticline with disequilibrium features implying that the deformation of this fold is ongoing at the present time. The accelerating emergence of this fold presumably counteracted a steepening of the regional gradient due to uplift of the mountain front to the north, and this would have reduced local gradients to account for the episodic reduction in sedimentation rate that we observe here (Figure 7). The Xiyu conglomerates clearly postdate this history of reduced sedimentation extending into the early Pleistocene.

5.2. Basal Age of the Xiyu Conglomerates in Neighboring Regions of Tian Shan

[30] As discussed above, controversy has surrounded the basal age of the Xiyu conglomerates in the Tian Shan region and arises from different prejudices concerning the factors controlling this massive conglomerate formation in NW China. The Xiyu conglomerate formation was originally assigned to a suite of typical massive molasse deposits, comprising dark-gray pebble to boulder conglomerates with minor interbeds of mudstone or sandstone in the base of the Dushanzi section in the northern Tian Shan [*Huang et al.*, 1947] where these conglomerates rest upon the underlying Neogene Dushanzi formation with clear unconformity as evidenced by remarkable difference in lithology and bedding attitudes. By lithologic correlation within the two Neogene depocenters of the Tarim Basin and southern margin of the Junggar Basin, the Xiyu conglomerates were classed as late Neogene molasse resting on the underlying

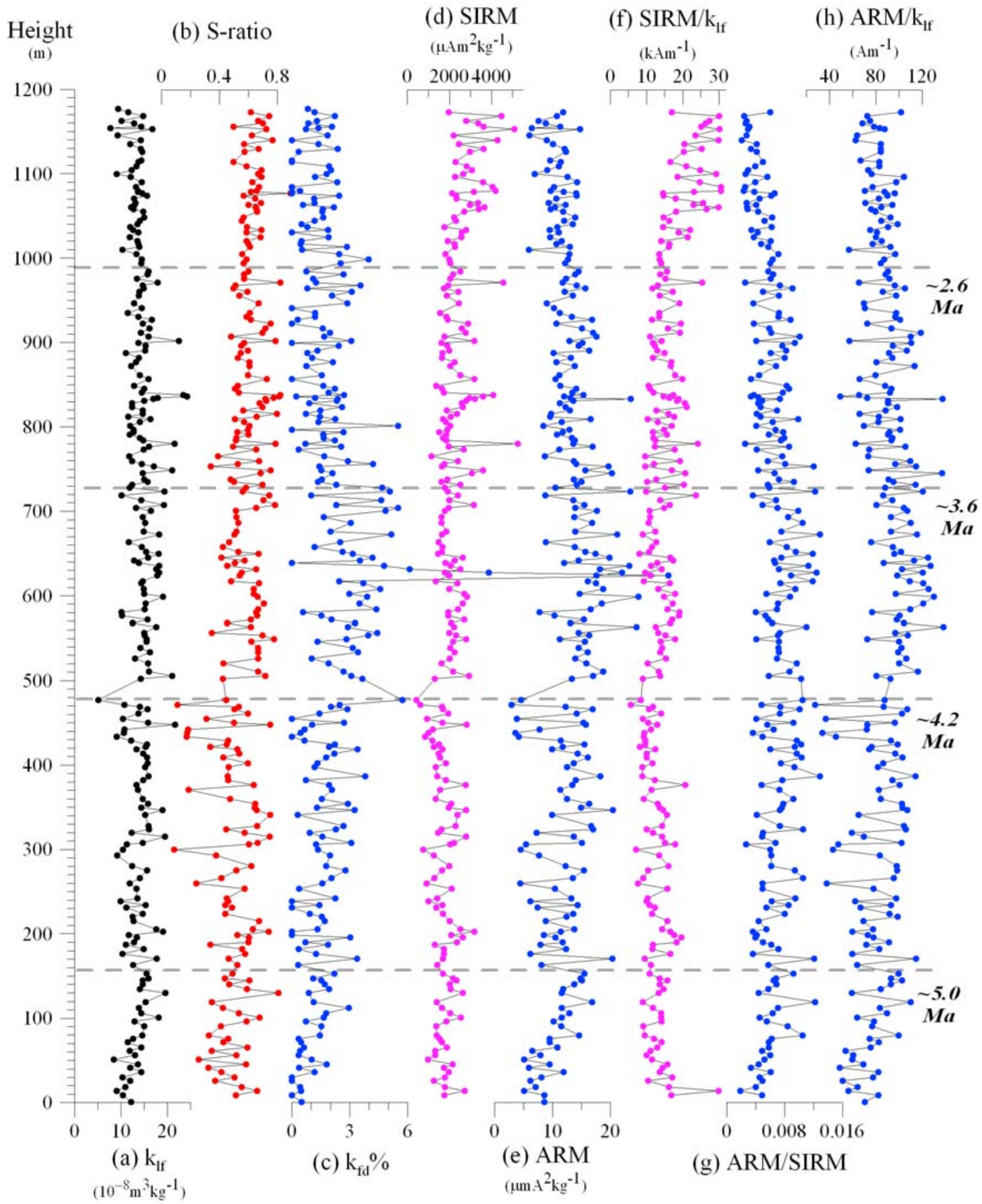

Figure 9. Rock magnetic results from the upper Yaha section in the Kuche Depression, NW China, comprising (a) low-frequency magnetic susceptibility (k_{lf}), (b) S ratio, (c) frequency magnetic susceptibility (k_{fd}%), (d) saturation isothermal remanent magnetization (SIRM), (e) anhysteresis remanent magnetization (ARM), (f) ratio of SIRM versus k_{lf}, (g) ratio of ARM versus SIRM, and (h) ratio of ARM versus k_{lf}. All parameters are shown as a function of height above the base of the sampled section.

Dushanzi, Kuche, and Atushi formations in southern Junggar, Kuche, and Kashi depressions with unconformity, paraconformity, or conformity, respectively [*Huang et al.*, 1947; *BGMRX*, 1993; *Jia et al.*, 2004]. Hence, the key problem for estimating commencement of deposition by magnetostratigraphy is whether or not there is a continuing contact between the Xiyu conglomerates and underlying strata. If a complete sequence of the above three formations is not found below the Xiyu conglomerates, there is most likely to be a sedimentation break with underlying strata in which case the magnetostratigraphic age for Xiyu conglomerate deposition will be overestimated.

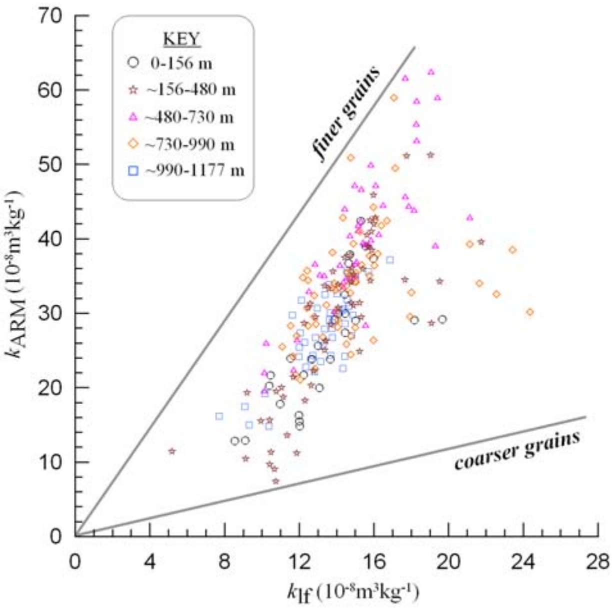

Figure 10. Variation in anhysteretic susceptibility (k_{ARM}) versus low-field susceptibility (k_{lf}) in the Neogene upper Yaha section [after *King et al.*, 1982]; the k_{ARM} versus k_{lf} plots do not discernibly emanate from the origin and indicate that relative grain size variations in magnetite content are significant in the middle part of the section ~156–990 m (~5.0–2.6 Ma).

[31] If deposition of this formation is climatically controlled a contemporaneous onset of deposition would be expected at around ~2.6 Ma in NW China, correlating with growth of continental ice sheets in high northern latitudes [*Sun et al.*, 2004, 2007]. In contrast, although there are uncertainties when there are possible time gaps between the Xiyu and underlying formations, it is clear that this definitive rudaceous suite has a diachronous basal contact [e.g., *Huang et al.*, 1947; *Li et al.*, 1979; *Burbank and Reynolds*, 1988; *Zheng et al.*, 2000; *Chen et al.*, 2002; *Sun et al.*, 2004; *Charreau et al.*, 2005, 2009; *Heermance et al.*, 2007, and this study]. Thus, magnetostratigraphic studies in the Kashi Basin show that the base of the Xiyu conglomerates varies by millions years: *Heermance et al.* [2007] identify basal ages ranging from 15.5 ± 0.5 Ma at the northernmost part of the foreland where Xiyu conglomerates lie in contact with the Miocene Wuqia Group, to 8.6 ± 0.1 Ma in the central part of the foreland and to 1.9 ± 0.2, ~1.04 and 0.7 ± 0.1 Ma along the southern deformation front of the foreland basin. Magnetostratigraphic studies on several sections with clear continuity between the Xiyu conglomerates and the underlying late Neogene formations (Atushi or Dushanzi formation) identify variable ages between ~3.8 Ma and ~1.95 Ma for the base of Xiyu conglomerate deposition [*Zheng et al.*, 2000; *Chen et al.*, 2002; *Sun et al.*, 2004; *Charreau et al.*, 2005; *Sun and Zhang*, 2009]. Commencement of Xiyu conglomerate deposition in the Kuitun He section is still in dispute [*Sun et al.*, 2004, 2007; *Charreau et al.*, 2005, 2008] although since the field boundary with the underlying Dushanzi formation is fixed, these different interpretations arise from contrasting correlations with the GPTS. The appearance of the Mammalian fossil *Equus sanmeniensis* near the base of the Xiyu conglomerates in the neighboring Anjihai section supports an early Pleistocene age in the northern Tian Shan [*Sun et al.*, 2007]. In the Yaha section, the clear conformable contact between the Xiyu conglomerates and underlying strata (Figures 2c and 2d), the well constructed polarity sequence correlating to the ATNTS2004 GPTS [*Lourens et al.*, 2004], and the compatible magnetostratigraphic ages for the superimposed part of our section with the top ~77 m of the section studied by *Charreau et al.* [2006] (Figure 3 and corresponding analysis in section 3) all collectively indicate that these Xiyu conglomerates have an early Pleistocene age of ~1.7 Ma. These conglomerates are thus best interpreted as a time-transgressive clastic wedge that propagated southward across the southern margin of the Tian Shan from a source region at the uplifted range front to the north [*Chen et al.*, 2002, 2007; *Heermance et al.*, 2007, 2008].

5.3. What Triggered the Formation of the Xiyu Conglomerates?

[32] The rock magnetic signatures in the upper Yaha section in the Kuche Depression (section 4, Figures 9 and 10) are evidently a composite signature of sedimentologic-tectonic and climatic factors, and the contributions of each are not simply isolated. The study section is located at the northern margin of the Taklimakan Desert in the Tarim Basin, the world's second largest shifting sand desert that began to form ~5.3 Ma ago, probably due to modification of atmospheric circulation patterns induced by uplift of the northern Tibetan Plateau [*Sun and Liu*, 2006; *Sun et al.*, 2008]. The growth of this desert would have produced intensified aridification and cooling, and accompanied modification of atmospheric circulation patterns in central Asia during the late Neogene [e.g., *An et al.*, 2001; *Guo et al.*, 2002; *Sun and Liu*, 2006; *Dupont-Nivet et al.*, 2007]. A specific signature here appears to be the influence of a warm/humid event during the period from ~5.0 to ~3.6 Ma characterized by higher fine-grained (i.e., SP, SD, and small PSD) ferromagnet inputs below the ~730 m level (Figures 9 and 10). In subsequent times, rock magnetic parameters imply a decreasing input of hematite of probable pedogenic origin accompanied by an increase in magnetite grain size fractions reflecting enhanced physical weathering as the climate cooled. Relatively, low-ferromagnet grain sizes observed during the early Pliocene interval are consistent with results of direct particle size analysis determined during the time interval between ~5.4 and 3.6 Ma in the Kuitun He section on the northern piedmont of the Tian Shan [*Sun et al.*, 2007], where they are attributed to the decreasing strength of the cold-dry winter monsoon in NW China during these times [e.g., *Guo et al.*, 2004; *Vandenberghe et al.*, 2004]. This warm and humid signature recognized from the upper Yaha section at ~5.0–3.6 Ma also corresponds with the record in neighboring regions in China [*Wu*, 2001; *Li et al.*, 2005; *Sun et al.*, 2007] and correlates with comparable events recognized in central Japan [*Wang et al.*, 2001] and in the sub-Himalayan region [*Hoorn et al.*, 2000]; it is broadly contemporaneous with a global eustatic sea level rise between ~5.8 and 4.0 Ma ago [*Hardenbol et al.*, 1998] when enhanced marine influences extending equitable climates into higher latitudes.

[33] Hence climate changes suggested by variations in rock magnetic properties within this section compare favorably with regional and global climate patterns during late Neogene times and are notably similar to the climate record in the neighboring Kuitun He on the northern piedmont of the Tian Shan [*Sun et al.*, 2007]. However, the contrasting ages for commencement of Xiyu conglomerate deposition in these two sections located on different flanks of the Tian Shan and separated by a N–S distance of ~260 km (Figure 1a) clearly show that formation of the Xiyu conglomerates in the foreland basins of the Tian Shan is essentially independent of climate although climatic influences will no doubt have modulated local accumulation rates. Noting that mountain uplift is generally coupled with subsidence of the adjoining foreland basin, and controlled by increased topographic gradient, transport energy and bedrock denudation rates, we consider that formation of the Xiyu conglomerates in the foreland basins of the Tian Shan is the signature of major regional uplift and denudation that produced a widespread time-transgressive clastic wedge.

6. Conclusions

[34] Detailed lithologic examination and magnetostratigraphic study of the youngest part of the Yaha succession beneath the Xiyu conglomerates formation in the Kuche Depression of the Tarim Basin has identified nine reversed and eight normal well-determined geomagnetic polarity zones dated ~5.3 to ~1.7 Ma by correlation with the ATNTS2004 GPTS [*Lourens et al.*, 2004]. The studied section overlaps and succeeds a section investigated by *Charreau et al.* [2006] and completes a regional magnetostratigraphy embracing the interval ~12.6–1.7 Ma. Deposition of the succession included within this study embraces syntectonic growth strata and shows an episodic fall in sedimentation rate from ~49 cm/kyr to ~24 cm/kyr prior to emplacement of the Xiyu conglomerates at ~1.7 Ma; this reduction in sedimentation is attributed to accelerated growth of the Qiulitage anticline and decrease in local topographic gradients. Rock magnetic parameters within the succession record a range of climatic and sedimentologic-tectonic signatures; the climatic signature identifies an early Pliocene warm and humid interval followed by increasing cooling and desertification which appears to have become most prominent after ~2.6 Ma.

[35] Estimates for the time of initiation of the Xiyu conglomerate formation now range from mid-Miocene to <1.0 Ma in different parts of the Tian Shan [*Teng et al.*, 1996; *Burchfiel et al.*, 1999; *Zheng et al.*, 2000; *Chen et al.*, 2002; *Sun et al.*, 2004; *Charreau et al.*, 2005, 2009; *Heermance et al.*, 2007; *Sun and Zhang*, 2009, and this study] and identify this prominent regional rock unit as a diverse and strongly diachronous formation. The variable ages of emplacement extending well into the Pleistocene epoch show that it cannot be climatically controlled. Instead, we consider that it is primarily a response to late tectonic reactivation in the Tian Shan.

[36] **Acknowledgments.** This study was financed by the National NSF of China (grants 40525013, 40821091). Dongjiang Sun, Qiang Li, and Anjiang Song are indebted for their contributions to the field sampling, and Chenglong Deng is acknowledged for valuable discussions. We are grateful to the Editor and two anonymous reviewers for their valuable comments which have materially improved the paper.

References

An, Z., J. E. Kutzbach, W. L. Prell, and S. C. Porter (2001), Evolution of Asian monsoons and phased uplift of the Himalaya-Tibetan plateau since late Miocene times, *Nature*, *411*, 62–66, doi:10.1038/35075035.

Avouac, J. P., P. Tapponnier, M. Bai, Y. Hou, and G. Wang (1993), Active thrusting and folding along the northeastern Tienshan, and rotation of Tarim relative to Dzungaria and Kazakahstan, *J. Geophys. Res.*, *98*, 6755–6804, doi:10.1029/92JB01963.

Balsam, W., J. Ji, and J. Chen (2004), Climatic interpretation of the Luochuan and Lintai loess sections, China, based on changing iron oxide mineralogy and magnetic susceptibility, *Earth Planet. Sci. Lett.*, *223*, 335–348, doi:10.1016/j.epsl.2004.04.023.

Bullen, M. E., D. W. Burbank, J. I. Garver, and K. Y. Abdrakhmatov (2001), Late Cenozoic tectonic evolution of the northwestern Tien Shan: New age estimates for the initiation of mountain building, *Geol. Soc. Am. Bull.*, *113*(12), 1544–1559, doi:10.1130/0016-7606(2001)113<1544:LCTEOT>2.0.CO;2.

Bullen, M. E., D. W. Burbank, and J. I. Garver (2003), Building the northern Tien Shan: Integrated thermal, structural, and topographic constraints, *J. Geol.*, *111*, 149–165, doi:10.1086/345840.

Burbank, D. W., and R. G. H. Reynolds (1988), Stratigraphic keys to the timing of thrusting in terrestrial foreland basins: Applications to the northwestern Himalaya, in *New Perspectives in Basin Analysis*, edited by K. L. Kleinspehn and C. Paola, pp. 332–351, Springer, New York.

Burbank, D. W., J. Verges, J. A. Munoz, and P. Bentham (1992), Coeval hindward- and forward-imbricating thrusting in the south-central Pyrenees, Spain: Timing and rates of shortening and deposition, *Geol. Soc. Am. Bull.*, *104*, 3–17, doi:10.1130/0016-7606(1992)104<0003:CHAFIT>2.3.CO;2.

Burbank, D., A. Meigs, and N. Brozovic (1996), Interaction of growing folds and coeval depositional systems, *Basin Res.*, *8*, 199–223, doi:10.1046/j.1365-2117.1996.00181.x.

Burchfiel, B. C., E. T. Brown, Q. Deng, X. Fang, P. Molnar, J. Shi, W. Zhangming, and Y. Huichan (1999), Crustal shortening on the margins of the Tian Shan, Xinjiang, China, *Int. Geol. Rev.*, *41*, 663–700, doi:10.1080/00206819909465164.

Bureau of Geology and Mineral Resources of Xinjiang Autonomous Region (BGMRX) (1993), *Regional Geology of Xinjiang Autonomous Region*, *Geol.Mem. Ser.*, vol. 1, 841 pp., Geol. Publ. House, Beijing.

Charreau, J., Y. Chen, S. Gilder, S. Dominguez, J.-P. Avouac, S. Sen, D. J. Sun, Y. A. Li, and W. M. Wang (2005), Magnetostratigraphy and rock magnetism of the Neogene Kuitun He section (northwest China): Implications for Late Cenozoic uplift of the Tianshan mountains, *Earth Planet. Sci. Lett.*, *230*, 177–192, doi:10.1016/j.epsl.2004.11.002.

Charreau, J., S. Gilder, Y. Chen, S. Dominguez, J.-P. Avouac, S. Sen, M. Jolivet, Y. Li, and W. Wang (2006), Magnetostratigraphy of the Yaha section, Tarim Basin (China): 11 Ma acceleration in erosion and uplift of the Tian Shan mountains, *Geology*, *34*(3), 181–184, doi:10.1130/G22106.1.

Charreau, J., J. Sun, Y. Chen, S. Gilder, B. Huang, and Q. Wang (2008), Addendum to "Late Cenozoic magnetostratigraphy and paleoenvironmental changes in the northern foreland basin of the Tian Shan Mountains" by Jimin Sun, Qinghai Xu, and Baochun Huang, *J. Geophys. Res.*, *113*, B06103, doi:10.1029/2007JB005489.

Charreau, J., et al. (2009), Neogene uplift of the Tian Shan Mountains observed in the magnetic record of the Jingou River section (northwest China), *Tectonics*, *28*, TC2008, doi:10.1029/2007TC002137.

Chen, J., D. W. Burbank, K. M. Scharer, E. Sobel, J. H. Yin, C. Rubin, and R. B. Zhao (2002), Magnetochronology of the Upper Cenozoic strata in the southwestern Chinese Tian Shan: Rates of Pleistocene folding and thrusting, *Earth Planet. Sci. Lett.*, *195*, 113–130, doi:10.1016/S0012-821X(01)00579-9.

Chen, J., R. Heermance, K. M. Scharer, D. W. Burbank, J. Miao, and C. S. Wang (2007), Quantification of growth and lateral propagation of the Kashi anticline, Southwest Chinese Tian Shan, *J. Geophys. Res.*, *112*, B03S16, doi:10.1029/2006JB004345.

Dearing, J. A., R. J. L. Dann, K. Hay, J. A. Lees, P. J. Loveland, B. A. Maher, and K. O'Grady (1966), Frequency-dependent susceptibility measurements of environmental materials, *Geophys. J. Int.*, *124*, 228–240, doi:10.1111/j.1365-246X.1996.tb06366.x.

Dumitru, T. A., D. Zhou, E. Z. Chang, S. A. Graham, M. S. Hendrix, E. R. Sobel, and A. R. Carroll (2001), Uplift, exhumation, and deformation in the Chinese Tian Shan, in *Paleozoic and Mesozoic Tectonic Evolution of Central Asia: From Continental Assembly to Intracontinental Deformation*, edited by M. S. Hendrix and G. A. Davis, pp., *Mem. Geol. Soc. Am.*, *194*, 71–99.

Dupont-Nivet, G., W. Krijgsman, C. G. Langereis, H. A. Abels, S. Dai, and X. M. Fang (2007), Tibetan plateau aridification linked to global cooling at the Eocene-Oligocene transition, *Nature*, *445*, 635–638, doi:10.1038/nature05516.

Fu, B., A. Lin, K.-I. Kano, T. Maruyama, J. Guo, and K. Y. Abdrakhmatov (2003), Quaternary folding of the eastern Tian Shan, northwest China, *Tectonophysics*, *369*, 79–101, doi:10.1016/S0040-1951(03)00137-9.

Gao, J., M. S. Li, X. C. Xiao, Y. Q. Tang, and G. Q. He (1998), Paleozoic tectonic evolution of the Tianshan Orogen, northwestern China, *Tectonophysics*, *287*, 213–231, doi:10.1016/S0040-1951(97)00211-4.

Gradstein, F. M., , J. G. Ogg, and A. G. Smith (Eds.) (2004), *A Geologic Time Scale 2004*, 589 pp., Cambridge Univ. Press, Cambridge, U. K.

Guo, Z. T., W. F. Ruddiman, Q. Z. Hao, H. B. Wu, Y. S. Qiao, R. X. Zhu, S. Z. Peng, J. J. Wei, B. Y. Yuan, and T. S. Liu (2002), Onset of Asian desertification by 22 Myr ago inferred from loess deposits in China, *Nature*, *416*, 159–163, doi:10.1038/416159a.

Guo, Z. T., S. Z. Peng, Q. Z. Hao, P. E. Biscaye, Z. S. An, and T. S. Liu (2004), Late Miocene-Pliocene development of Asian aridification as recorded in the Red-Earth Formation in northern China, *Global Planet. Change*, *41*, 135–145, doi:10.1016/j.gloplacha.2004.01.002.

Hardenbol, J., J. Thierry, M. B. Farley, T. Jacquin, P. C. De Graciansky, and P. R. Vail (1998), Mesozoic and Cenozoic sequence chronostratigraphic framework of European basins, *SEPM Spec. Publ.*, *60*, 3–13.

Harrison, T. M., P. Copeland, S. A. Hall, J. Quade, S. Burner, T. P. Ojha, and W. S. F. Kidd (1993), Isotopic preservation of Himalayan/Tibetan uplift, denudation, and climate histories of two molasses deposits, *J. Geol.*, *100*, 157–175, doi:10.1086/648214.

Heermance, R. V., J. Chen, D. W. Burbank, and C. S. Wang (2007), Chronology and tectonic controls of Late Tertiary deposition in the southwestern Tian Shan foreland, NW China, *Basin Res.*, *19*, 599–632, doi:10.1111/j.1365-2117.2007.00339.x.

Heermance, R. V., J. Chen, D. B. Burbank, and J. Miao (2008), Temporal constraints and evidence for pulsed Late Cenozoic deformation during the structural disruption of the active Kashi foreland, northwest China, *Tectonics*, *27*, TC6012, doi:10.1029/2007TC002226.

Hendrix, M., T. Damitru, and S. Graham (1994), Late Oligocene–early Miocene unroofing in the Chinese Tian Shan: An early effect of the India-Asia collision, *Geology*, *22*, 487–490, doi:10.1130/0091-7613(1994)022<0487:LOEMUI>2.3.CO;2.

Hoorn, C., T. Ohja, and J. Quade (2000), Palynological evidence for vegetation development and climatic change in the Sub-Himalayan Zone (Neogene, Central Nepal), *Palaeogeogr. Palaeoclimatol. Palaeoecol.*, *163*, 133–161, doi:10.1016/S0031-0182(00)00149-8.

Huang, B., Y. Wang, T. Liu, T. Yang, Y. Li, D. Sun, and R. Zhu (2004), Paleomagnetism of Miocene sediments from the Turfan Basin, Northwest China: No significant vertical-axis rotation during neotectonic compression within the Tian Shan Range, central Asia, *Tectonophysics*, *384*, 1–21, doi:10.1016/j.tecto.2004.01.003.

Huang, B., J. D. A. Piper, S. Peng, T. Liu, Z. Li, Q. Wang, and R. Zhu (2006), Magnetostratigraphic and rock magnetic constraints on the history of Cenozoic uplift of the Chinese Tian Shan, *Earth Planet. Sci. Lett.*, *251*, 346–364, doi:10.1016/j.epsl.2006.09.020.

Huang, B., J. D. A. Piper, and R. Zhu (2008), Reply to the comment by J. Charreau et al. on "Magnetostratigraphic study of the Kuche Depression, Tarim Basin, and Cenozoic uplift of the Tian Shan Range, Western China" [*Earth Planet. Sci. Lett.*, 2008, doi: 10.1016/j.epsl.2008.01.025], *Earth Planet. Sci. Lett.*, *275*, 404–406, doi: 10.1016/j.epsl.2008.06.053.

Huang, J., Z. Yang, Y. Cheng, Z. Zhou, M. Bian, and W. Weng (1947), Geological report about petroleum in Xinjiang, *Spec. Geol. Rep.*, *21*, 31–66.

Hubert-Ferrari, A., J. Suppe, R. Gonzalez-Mieres, and X. Wang (2007), Mechanisms of active folding of the landscape (southern Tian Shan, China), *J. Geophys. Res.*, *112*, B03S09, doi:10.1029/2006JB004362.

Ji, J., P. Luo, P. White, H. Jiang, L. Gao, and Z. Ding (2008), Episodic uplift of the Tianshan Mountains since the late Oligocene constrained by magnetostratigraphy of the Jingou River section, in the southern margin of the Junggar Basin, China, *J. Geophys. Res.*, *113*, B05102, doi:10.1029/2007JB005064.

Jia, C., S. Zhang, and S. Wu (Eds.) (2004), *Stratigraphy of the Tarim Basin and Adjacent Areas*, (in Chinese), 1063 pp., Science Press, Beijing.

King, J., S. K. Banerjee, J. Marvin, and Ö. Özdemir (1982), A comparison of different magnetic methods for determining the relative grain size of magnetite in natural materials: Some results from lake sediments, *Earth Planet. Sci. Lett.*, *59*, 404–419, doi:10.1016/0012-821X(82)90142-X.

Kirschvink, J. L. (1980), The least squares line and plane and the analysis of paleomagnetic data, *Geophys. J. R. Astron. Soc.*, *62*, 699–712.

Li, J., S. Wen, Q. Zhang, F. Wang, B. Zheng, and B. Li (1979), A discussion on the period, amplitude and type of the uplift of the Qinghai-Xizang Plateau, *Sci. China, Ser. A*, *22*(11), 1314–1328.

Li, J., L. Wang, Y. P. Pei, and S. Z. Peng (2005), Ecological changes during 6.2–2.4 Ma revealed by palynological record from Red Clay Deposits in the Loess Plateau and implications for paleoclimatic evolution, *Quat. Sci.*, *25*, 467–473.

Lourens, L., F. Hilgen, N. J. Shackleton, J. Laskar, and J. Wilson (2004), Orbital tuning calibrations and conversions for the Neogene Period, in *A Geologic Time Scale 2004*, edited by F. M. Gradstein, J. G. Ogg, and A. G. Smith, pp. 469–484, Cambridge Univ. Press, Cambridge, U. K.

McFadden, P. L., and M. W. McElhinny (1990), Classification of the reversal test in palaeomagnetism, *Geophys. J. Int.*, *103*, 725–729, doi:10.1111/j.1365-246X.1990.tb05683.x.

Métivier, F., and Y. Gaudemer (1997), Mass transfer between eastern Tien Shan and adjacent basins (central Asia): Constraints on regional tectonics, *Geophys. J. Int.*, *128*, 1–17, doi:10.1111/j.1365-246X.1997.tb04068.x.

Molnar, P., and P. Tapponnier (1975), Cenozoic tectonics of Asia: Effects of continental collision, *Science*, *189*, 419–426, doi:10.1126/science.189.4201.419.

Parés, J. M. (2004), How deformed are weakly deformed mudrocks? Insights from magnetic anisotropy, in *Magnetic Fabrics: Methods and Applications*, edited by F. Martin-Hernàndez et al., Geol. Soc. Spec. Publ., *238*, 191–203.

Patriat, P., and J. Achache (1984), India-Eurasia collision chronology has implications for crustal shortening and driving mechanism of plates, *Nature*, *311*, 615–621, doi:10.1038/311615a0.

Sobel, E. R., and T. A. Dumitru (1997), Thrusting and exhumation around the margins of the western Tarim basin during the India-Asia collision, *J. Geophys. Res.*, *102*, 5043–5063, doi:10.1029/96JB03267.

Sobel, E. R., M. Oskin, D. Burbank, and A. Mikolaichuk (2006), Exhumation of basement-cored uplifts: Example of the Kyrgyz Range quantified with apatite fission track thermochronology, *Tectonics*, *25*, TC2008, doi:10.1029/2005TC001809.

Sun, J. M., and T. S. Liu (2006), The age of the Taklimakan Desert, *Science*, *312*, 1621, doi:10.1126/science.1124616.

Sun, J. M, and Z. Q. Zhang (2009), Syntectonic growth strata and implications for late Cenozoic tectonic uplift in the northern Tian Shan, China, *Tectonophysics*, *463*, 60–68, doi:10.1016/j.tecto.2008.09.008.

Sun, J. M., R. X. Zhu, and J. Bowler (2004), Timing of the Tianshan Mountains uplift constrained by magnetostratigraphic analysis of molasses deposits, *Earth Planet. Sci. Lett.*, *219*, 239–253, doi:10.1016/S0012-821X(04)00008-1.

Sun, J. M., Q. H. Xu, and B. C. Huang (2007), Late Cenozoic magnetochronology and paleoenvironmental changes in the northern foreland basin of the Tianshan Mountains, *J. Geophys. Res.*, *112*, B04101, doi:10.1029/2006JB004653.

Sun, J. M., L. Y. Zhang, C. L. Deng, and R. X. Zhu (2008), Evidence for enhanced aridity in the Tarim basin of China since 5.3 Ma, *Quat. Sci. Rev.*, *27*, 1012–1023, doi:10.1016/j.quascirev.2008.01.011.

Tapponnier, P., and P. Molnar (1979), Active faulting and Cenozoic tectonics of the Tien Shan, Mongolia and Baykal regions, *J. Geophys. Res.*, *84*, 3425–3459, doi:10.1029/JB084iB07p03425.

Tarling, D. H. and F. Hrouda (Eds.) (1993), *The Magnetic Anisotropy of Rocks*, 217 pp., Chapman and Hall, London.

Teng, Z. H., L. P. Yue, R. H. Pu, X. Q. Deng, and X. W. Bian (1996), The magnetostratigraphic age of the Xiyu Formation, *Geol. Rev.*, *42*, 481–489.

Vandenberghe, J., H. Y. Lu, D. H. Sun, J. Huissteden, and M. Konert (2004), The late Miocene and Pliocene climate in East Asia as recorded by grain size and magnetic susceptibility of the Red Clay deposits (Chinese Loess Plateau), *Palaeogeogr. Palaeoclimatol. Palaeoecol.*, *204*, 239–255, doi:10.1016/S0031-0182(03)00729-6.

Wang, W. M., T. Saito, and T. Nakagawa (2001), Palynostratigraphy and climatic implications of Neogene deposits in the Himi area of Toyama Prefecture, Central Japan, *Rev. Palaeobot. Palynol.*, *117*, 195–281, doi:10.1016/S0034-6667(01)00097-5.

Windley, B. F., M. B. Allen, C. Zhang, Z. Y. Zhao, and G. R. Wang (1990), Paleozoic accretion and Cenozoic redeformation of the Chinese Tianshan Range, central Asia, *Geology*, *18*, 128–131, doi:10.1130/0091-7613(1990)018<0128:PAACRO>2.3.CO;2.

Wu, Y. S. (2001), Palynoflora at late Miocene-early Pliocene from Leijiahe of Lintai, Gansu Province, China, *Acta Bot. Sin.*, *43*, 750–756.

Yin, A., S. Nie, P. Craig, T. M. Harrison, F. J. Ryerson, X. Qian, and G. Yang (1998), Late Cenozoic Tectonic evolution of the southern Chinese Tian Shan, *Tectonics*, *17*, 1–27, doi:10.1029/97TC03140.

Zhang, P., P. Molnar, and W. Downs (2001), Increased sedimentation rates and grain sizes 2–4 Myr ago due to the influence of climate change on erosion rates, *Nature*, *410*, 891–897, doi:10.1038/35069099.

Zheng, H. B., C. M. Powell, Z. An, J. Zhou, and G. Dong (2000), Pliocene uplift of the northern Tibetan Plateau, *Geology*, *28*, 715–718, doi:10.1130/0091-7613(2000)28<715:PUOTNT>2.0.CO;2.

Zijderveld, J. D. A. (1967), A.C. demagnetization of rocks: Analysis of results, in *Methods in Paleomagnetism*, edited by D. W. Collinson et al., pp. 254–286, Elsevier Sci., New York.

B. Huang, Q. Qiao, H. Wang, and C. Zhang, Paleomagnetism and Geochronology Laboratory of the State Key Laboratory of Lithospheric Evolution, Institute of Geology and Geophysics, Chinese Academy of Sciences, Beijing 100029, China. (bchuang@mail.iggcas.ac.cn)

J. D. A. Piper, Geomagnetism Laboratory, Department of Earth and Ocean Sciences, University of Liverpool, Liverpool L69 7ZE, UK.